Journal of Medicinal Chemistry

Article

pubs.acs.org/jmc

Molecular Systems Pharmacology: Isoelectric Focusing Signature of Protein Kinase Cδ Provides an Integrated Measure of Its Modulation in Response to Ligands

Noemi Kedei,[†,⊥] Jin-Qiu Chen,[‡,⊥] Michelle A. Herrmann,[‡] Andrea Telek,[†] Paul K. Goldsmith,[§] Mark E. Petersen,[∥] Gary E. Keck,[∥] and Peter M. Blumberg*[,†]

[†]Laboratory of Cancer Biology and Genetics, [‡]Collaborative Protein Technology Resource, Laboratory of Cell Biology, and [§]Office of Science and Technology Partnerships, Center for Cancer Research, National Cancer Institute, Bethesda, Maryland 20892, United States

[∥]Department of Chemistry, University of Utah, Salt Lake City, Utah 84112, United States

Supporting Information

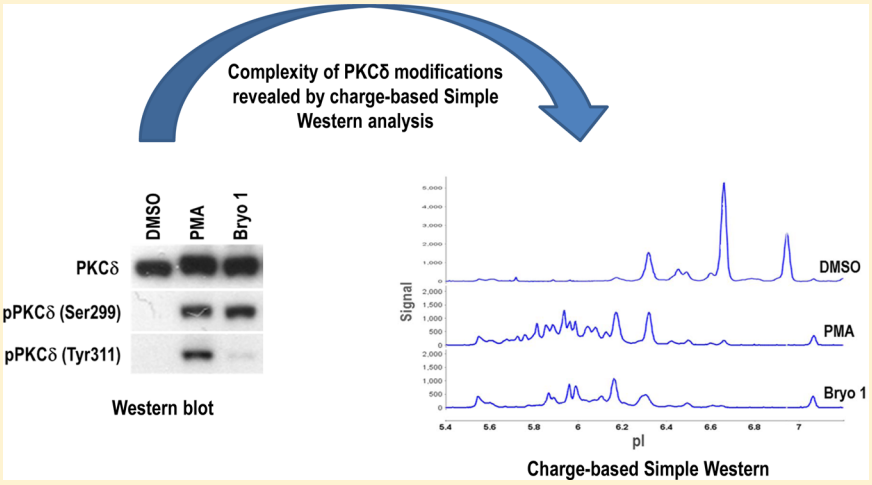

ABSTRACT: Protein kinase C (PKC), a validated therapeutic target for cancer chemotherapy, provides a paradigm for assessing structure−activity relations, where ligand binding has multiple consequences for a target. For PKC, ligand binding controls not only PKC activation and multiple phosphorylations but also subcellular localization, affecting subsequent signaling. Using a capillary isoelectric focusing immunoassay system, we could visualize a high resolution isoelectric focusing signature of PKCδ upon stimulation by ligands of the phorbol ester and bryostatin classes. Derivatives that possessed different physicochemical characteristics and induced different patterns of biological response generated different signatures. Consistent with different patterns of PKCδ localization as one factor linked to these different signatures, we found different signatures for activated PKCδ from the nuclear and non-nuclear fractions. We conclude that the capillary isoelectric focusing immunoassay system may provide a window into the integrated consequences of ligand binding and thus afford a powerful platform for compound development.

INTRODUCTION

A challenge in medicinal chemistry is the appropriate evaluation of structure−activity relations. If the assays fail to fully capture the critical features determining biological activity, then the impact from the synthetic effort is correspondingly diminished. The traditional model of drug action is of a ligand binding to a drug target, with response linked to target occupancy. The profound progress in our understanding of cellular biochemistry now affords detailed, albeit still developing, insights into the complexity of regulation of individual drug targets. Incorporating these insights into the evaluation of structural analogues promises new opportunities for enhancing efficiency in drug development. This concept of molecular systems pharmacology, probing contextual structure−activity relationships (CSARs), is illustrated here for a particular therapeutic target, protein kinase Cδ (PKCδ), which displays complex regulation in response to ligands directed at its regulatory C1 domain.[1,2] We show that a series of ligands for the regulatory domain of PKCδ are not equivalent but can be distinguished by the isoelectric focusing signatures of PKCδ that they induce, as detected by a capillary isoelectric focusing immunoassay system. In this system, proteins and their phosphorylated isoforms are separated by charge, followed by target specific

Received: March 17, 2014
Published: May 24, 2014

   dx.doi.org/10.1021/jm500417b | J. Med. Chem. 2014, 57, 5356−5369

antibody probing and chemiluminescence detection. Multiple phosphorylation isoforms can be simultaneously separated, detected, and quantified allowing fine dissection of molecular signaling events.

PKC plays a central role in cellular signaling, responding to the lipophilic second messenger *sn*-1,2-diacylglycerol (DAG), and is a validated therapeutic target for cancer and a range of other conditions.[3] DAG, which is generated as one of the products of phosphoinositide turnover in response to activation of a wide variety of cellular receptors, binds to the C1 domains of PKC. The C1 domains function as hydrophobic switches.[4,5] They possess a hydrophobic surface interrupted by a hydrophilic cleft. The DAG, ultrapotent surrogates such as the phorbol esters, or synthetic ligands such as DAG-lactones[6] or benzolactams[7] insert into this hydrophilic cleft, completing the hydrophobic surface as well as providing additional hydrophobic structural elements. Driven by this increase in hydrophobicity, the C1 domain–ligand complex associates with the membrane, bringing about conformational change in the PKC leading to enzymatic activation and a shift in its subcellular localization.

Both the pattern of membrane localization and the kinetics of the shift in localization markedly depend on the structure of the ligand. More lipophilic ligands, such as phorbol 12-myristate 13-acetate (PMA), initially cause PKCδ to move to the plasma membrane, after which it slowly shifts in part to internal membranes. More hydrophilic ligands, such as phorbol 12,13-dibutyrate, in contrast, cause the initial localization to the internal membranes.[8,9] The pattern of localization, moreover, correlates in part with the pattern of biological response. Thus, the tumor promoting derivative 12-deoxyphorbol 13-tetradecanoate behaves like PMA, whereas the antipromoting derivative 12-deoxyphorbol 13-phenylacetate acts like phorbol 12,13-dibutyrate.[8] Indirect evidence suggests that the influence of localization may be yet more complex. Marquez and co-workers evaluated, in a range of biological systems, combinatorial libraries of DAG-lactones that only varied in their hydrophobic substituents.[10] Virtually each biological assay revealed a different pattern of structural selectivity. The authors hypothesized that the varied hydrophobic moieties provided chemical "zip codes" to membrane subdomains, at a level of resolution beyond that revealed by imaging of GFP-tagged PKC constructs.

A further critical level of regulation for PKC is by phosphorylation (Figure 1),[11] where phosphorylation at

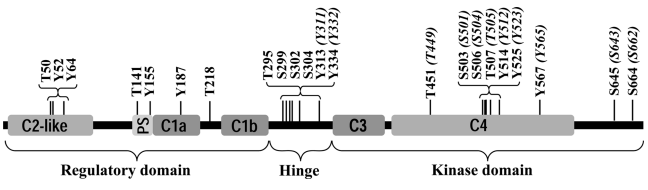

Figure 1. Sites of phosphorylation on PKCδ. Sites of phosphorylation on Ser/Thr and on Tyr of human PKCδ are indicated (numbering for the mouse/rat isoforms is in italic).[15,23−25,55]

serine/threonine sites in the activation loop, the turn motif, and the hydrophobic motif of the kinase domain are required for rendering the enzyme capable of being activated upon binding of ligands to its C1 regulatory domain, as well as controlling its stability within the cell.[12−15] Additional regulation, although not as well understood, is exerted by phosphorylation of tyrosine residues.[16−18] In the case of PKCδ, different tyrosine residues are required for the function of PKCδ for different biological end points. Thus, mutation to phenylalanine of tyrosine residues at positions 64 and 187 of PKCδ blocks its contribution to apoptosis of C6 glioma cells in response to etoposide, whereas mutation of residues at positions 52, 64, and 155 enhanced apoptosis of the C6 cells in response to Sindbis virus.[19,20] Additionally, phosphorylation at tyrosine 311 has been reported to change its selectivity for the substrate cardiac troponin I.[21,22] Multiple additional phosphorylation sites on PKCδ have been characterized (Figure 1).[23−25] Ser 299 is of particular interest in that it has been suggested that this site provides a marker of the enzymatically active PKCδ, as distinct from the enzyme simply being in a state capable of being activated by ligands.[23] For most of the sites of phosphorylation, however, neither is their regulatory impact known nor are reagents available for assessing their phosphorylation.

The pattern of PKCδ phosphorylation will necessarily reflect an integrated measure of ligand binding, conformational change, and colocalization with kinases such as PDK1, with tyrosine kinases such as Abl or Src, or with protein phosphatases such as PHLPP.[26,16] In elegant studies using FRET reporter constructs, Newton et al. showed marked differences in the level of phosphatase activity as a function of the particular membrane compartment.[27] Furthermore, the pattern of phosphorylation itself influences localization of PKCδ.[28]

In the present study, we direct particular attention to three PKC ligands with different biology. Although PKC isoforms are activated by binding of diacylglycerol, phorbol esters, and related ligands to their C1 domains, downstream consequences are not necessarily the same. Bryostatin 1 is a complex macrocyclic lactone that binds with high affinity to the same site on the C1 domain as do the phorbol esters, leading to enzymatic activation. Paradoxically, however, bryostatin 1 fails to induce many of the responses typical of the phorbol esters and, when added in combination with the phorbol ester, suppresses the phorbol ester response.[29,30] Of particular note, whereas the phorbol esters represent the paradigm for tumor promotion, bryostatin 1 fails to be tumor promoting and indeed suppresses the tumor promotion induced by phorbol ester.[31] Given the extensive involvement of PKC in cancer, bryostatin 1 is being extensively evaluated in cancer clinical trials. Exciting advances in the chemistry of the bryostatins are now making it possible to explore which structural features confer their unusual pattern of response. The bryostatin derivative Merle 23 has been of particular interest. In the U937 human leukemia cell line, the phorbol ester PMA induces attachment and inhibits proliferation; bryostatin 1 shows little effect in either assay and suppresses the action of PMA; the bryostatin derivative Merle 23 acts like PMA, highlighting the structural features that distinguish Merle 23 from bryostatin 1.[32] In the LNCaP human prostate cancer cell line, PMA induces tumor necrosis factor α (TNFα) secretion and inhibits cell growth; bryostatin 1 again shows little effect on either end point; Merle 23, in contrast to its behavior in the U937 cells, now acts more like bryostatin 1, showing reduced induction of TNFα secretion and little inhibition of cell growth.[33] Detailed analysis of its actions in the LNCaP cells, however, shows that Merle 23 may be more or less PMA-like in this system, depending on the specific response.

dx.doi.org/10.1021/jm500417b | J. Med. Chem. 2014, 57, 5356−5369

Single measures of ligand interaction with PKC, such as in vitro ligand binding or enzymatic activation, while a clear first level of characterization, necessarily cannot capture this degree of complexity found in the intact cell. Chromatographic fractionation of stimulated PKCδ by FPLC yields a broad profile, with different functional characteristics in different portions of the profile, but lacks resolution.[34] Western blotting of PKCδ with an pPKCδY311 antibody reveals that bryostatin 1 fails to induce phosphorylation at this site in LNCaP cells, unlike PMA, but addresses neither the absolute level of substitution at this site nor the status at the other sites of phosphorylation.[33] Here, we explore the potential of high resolution isoelectric focusing with immunoassay detection to provide a signature of the pattern of phosphorylation (or other charge altering modifications) of PKCδ as a function of ligand. Charge-based Simple Western technology is a capillary-based isoelectic focusing (IEF) immunoassay system, which employs high-resolution IEF separation of proteins by charge followed by target-specific immune-probing to simultaneously detect and quantify multiple protein phosphorylation (or other post-translational modification) isoforms. The charge-based Simple Western apparatus and associated software provide a robust platform for sample evaluation[35,36] and have the potential to detect signals that are not accessible by conventional Western blot.[37] Analyzing a series of ligands for PKC that differ in the patterns of response that they induce in the LNCaP human prostate cell line,[33,38] we show that these ligands likewise induce different isoelectric focusing signatures for PKCδ. The concept of function-oriented synthesis is that the modern medicinal chemist seeks to capture the relevant functional activity of a lead compound while reducing synthetic complexity.[39] For PKCδ, the isoelectric focusing signature provides an integrated window into the complex consequences of ligand binding and localization in the intact cell, as reflected in its pattern of regulatory phosphorylations or other modifications. This more detailed picture provides an additional layer of insight into contextual structure−activity relationships (CSARs) for PKCδ ligands. Such a signature has value even if, like a gene expression microarray, the individual elements contributing to the signature remain to be dissected.

RESULTS

Modest Differences in Regulation of PKCs by Ligands As Detected by Immunoblotting. Analysis by immunoblotting of PKCα and PKCδ in the LNCaP cells upon treatment for 30 min with PMA, bryostatin 1, and Merle 23 showed only modest differences (Figure 2), consistent with our findings as reported previously.[33] With all three ligands, PKCα showed a limited increase in staining for pT638, a regulatory phosphorylation in the turn motif.[12] PKCδ displayed a reduction in mobility together with phosphorylation detected with an antibody directed at pS299, a site associated with PKCδ activation.[23,13] As shown both by the similar intensities of the bands detected with the PKCδ antibody and by the lack of appearance of lower molecular weight forms (data not shown), proteolytic degradation of PKCδ was not evident under these conditions. In contrast to the similar effects of PMA, bryostatin 1, and Merle 23 on phosphorylation of PKCδ at S299, the three ligands had differential effects, as revealed by staining with an antibody directed at pY311, as previously reported.[33] Strong staining was seen with PMA, very little with bryostatin 1, and intermediate staining with Merle 23. Similar levels of ERK1/2 phosphorylation were observed with all three ligands, confirming that all three ligands were being used at effective concentrations. Because of different affinities of the different antibodies, the absolute levels of modification as detected by the various antibodies could not be compared.

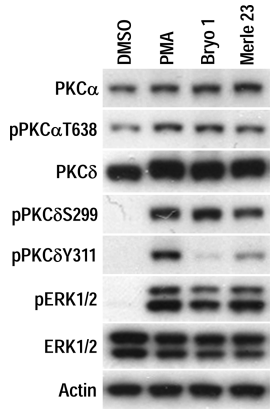

Figure 2. Changes in phosphorylation of PKCs in LNCaP cells. LNCaP cells were treated with PMA, bryostatin 1, or Merle 23 (1000 nM) for 30 min. Total cell lysates were prepared and evaluated by Western blotting with the indicated antibodies. The results are representative of three independent experiments.

Marked Differences in Regulation of PKCδ by Different Ligands As Detected by Charge-Based Simple Western Analysis. Charge-based Simple Western analysis of PKCδ revealed much greater complexity. By use of antibody directed against total PKCδ, a complex pattern of peaks was already evident for the DMSO control (Figure 3A). In the illustrated experiment, 38.8% of total PKCδ had a pI of 6.66 (peak 18), 19.2% and 17.35% had pI's of 6.31 and 6.94, respectively (peaks 13 and 19) and 10.1% had a pI of 6.61 (peak 17). As discussed below (see Figure 6), peak 18 is detected with antibodies directed against the phosphorylated activation loop (T505) and turn motifs (S643), and, based on its abundance as the major PKCδ peak in the absence of stimulation, it is plausibly the triphosphorylated PKCδ described as being the mature protein capable of activation (there was not a suitable antibody for the phosphorylated hydrophobic motif of PKCδ). Peak 19 is also phosphorylated at the activation loop and turn motifs. Because it has a higher pI (is less phosphorylated) than peak 18, it is possible that it is lacking phosphorylation on the hydrophobic motif. Peak 13, based on its pI, is more highly phosphorylated than is peak 18 and is detected with the antibody for pPKCδS299. It is most like the tetraphosphorylated PKCδ containing the activation loop, turn, and hydrophobic motif phosphorylations. This is not so clear in Figure 6 but is supported by other experiments in which peak 13 is more prominent. In any case, as emphasized in our discussion regarding Figure 6, considerable additional work will be required before the modifications responsible for the various peaks are fully identified.

Upon PMA treatment, there was a dramatic reduction in most of these baseline peaks and the emergence of a highly complex pattern at lower pI, consistent with phosphorylation of PKCδ. Although an overall similar pattern was observed upon treatment with bryostatin 1 or Merle 23 as was seen with PMA, closer examination revealed both the absence of some bands and the emergence of others (Figure 3A). For identification, peaks were numbered and their pI values indicated. The pattern of response was reproducible between different runs for the

dx.doi.org/10.1021/jm500417b | J. Med. Chem. 2014, 57, 5356−5369

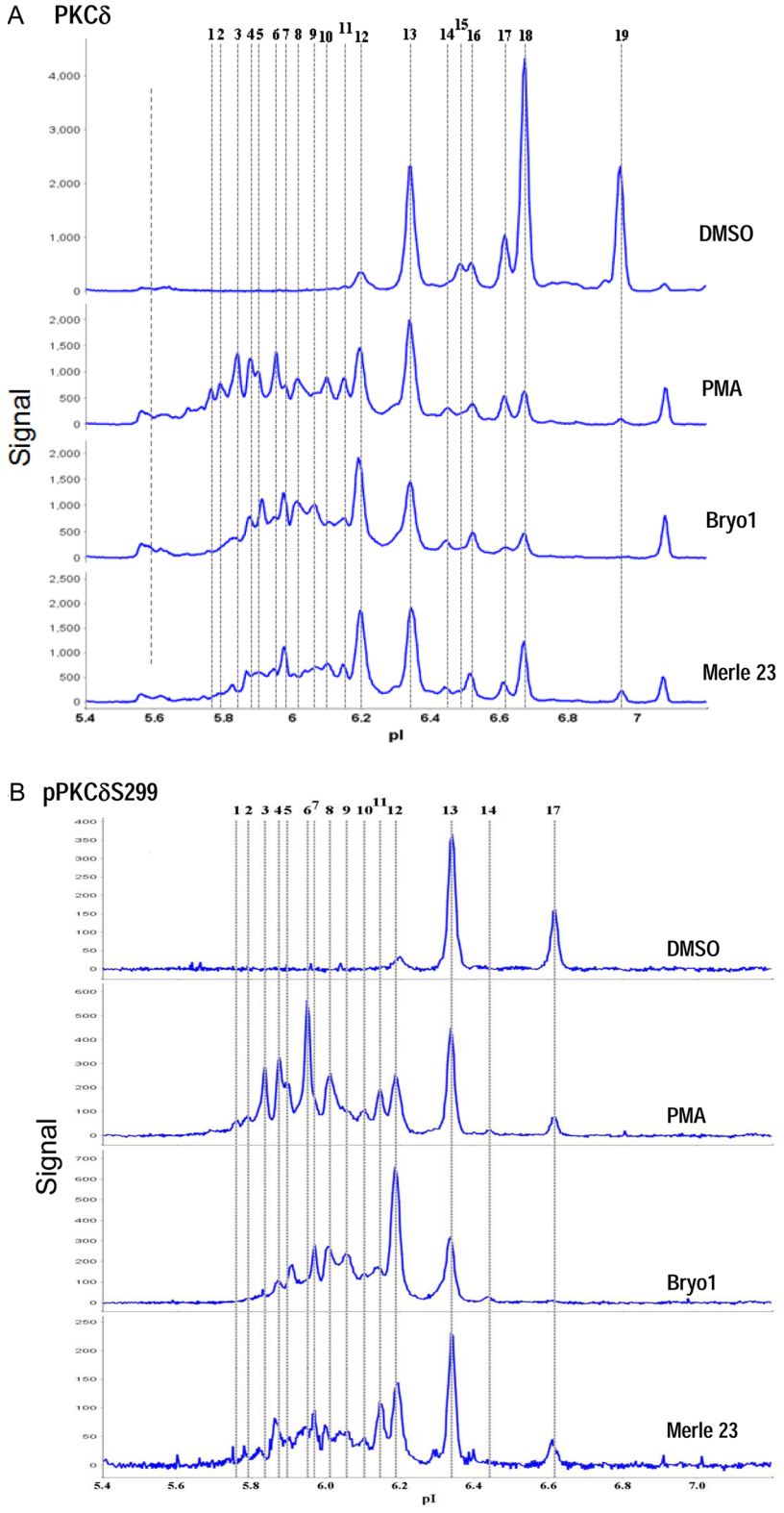

Figure 3. Complex pattern of PKCδ modification measured by the charge-based Simple Western system. LNCaP cells were treated with PMA, bryostatin 1, or Merle 23 (1000 nM) for 30 min. DMSO was the vehicle control. Total cell lysates were prepared as described in Experimental Section and evaluated by the charge-based Simple Western system using total PKCδ antibody (from Santa Cruz) (A) or pPKCδS299 antibody (B). The results are representative of three independent experiments. Peaks with different isoelectric focusing points (pI) were numbered for easier comparison between runs.

different treatments, but minor shifts in the pI values for the different peaks were observed and the region around peaks 8–10 showed more variability.

The above pattern was detected with an antibody that detects total PKCδ independent of its state of phosphorylation. We similarly compared the patterns using the pPKCδS299

dx.doi.org/10.1021/jm500417b | J. Med. Chem. 2014, 57, 5356–5369

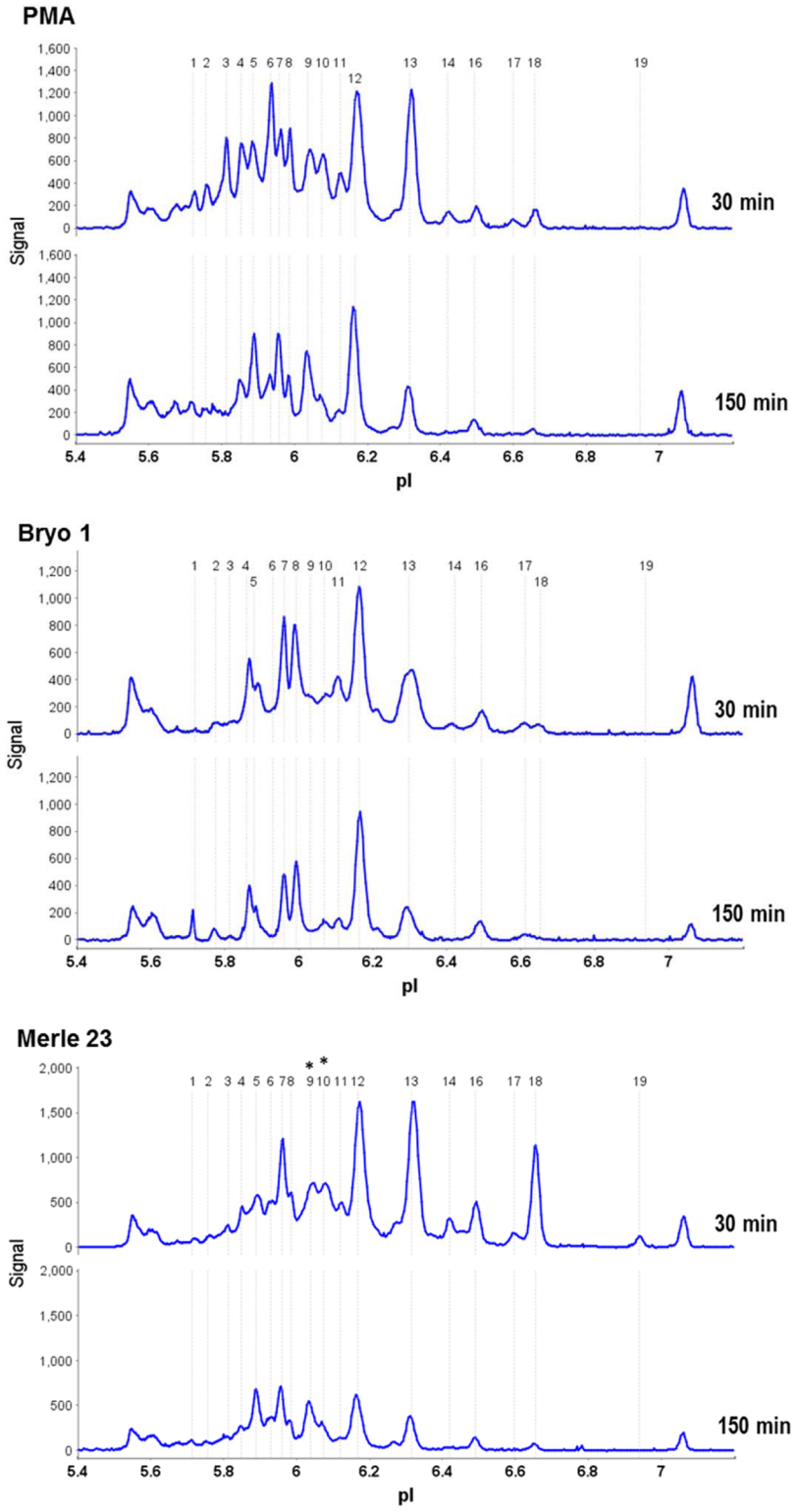

Figure 4. The pattern of PKCδ phosphorylation changes with time. LNCaP cells were treated with PMA, bryostatin 1, or Merle 23 (1000 nM) for 30 or 150 min. Total cell lysates were prepared and evaluated by the charge-based Simple Western system using total PKCδ antibody. The results are representative of three independent experiments. Asterisks denote that peaks 9 and 10 show variability compared to peaks labeled 9 and 10 in Figure 3.

antibody, which has been described as being selective for the active enzyme (Figure 3B). Here, the pattern is somewhat simplified, representing a subset of the bands detected with the antibody to total PKCδ, but the multiplicity of peaks is still dramatic. Comparison between the patterns with PMA, bryostatin 1, and Merle 23 reveals appreciable differences, with bryostatin 1 treatment leading to a relative deficiency in the more acidic bands seen with PMA, e.g., peak 3, and with Merle 23 yielding a pattern intermediate between that of bryostatin 1 and PMA. Differences in the relative abundance of

dx.doi.org/10.1021/jm500417b | J. Med. Chem. 2014, 57, 5356−5369

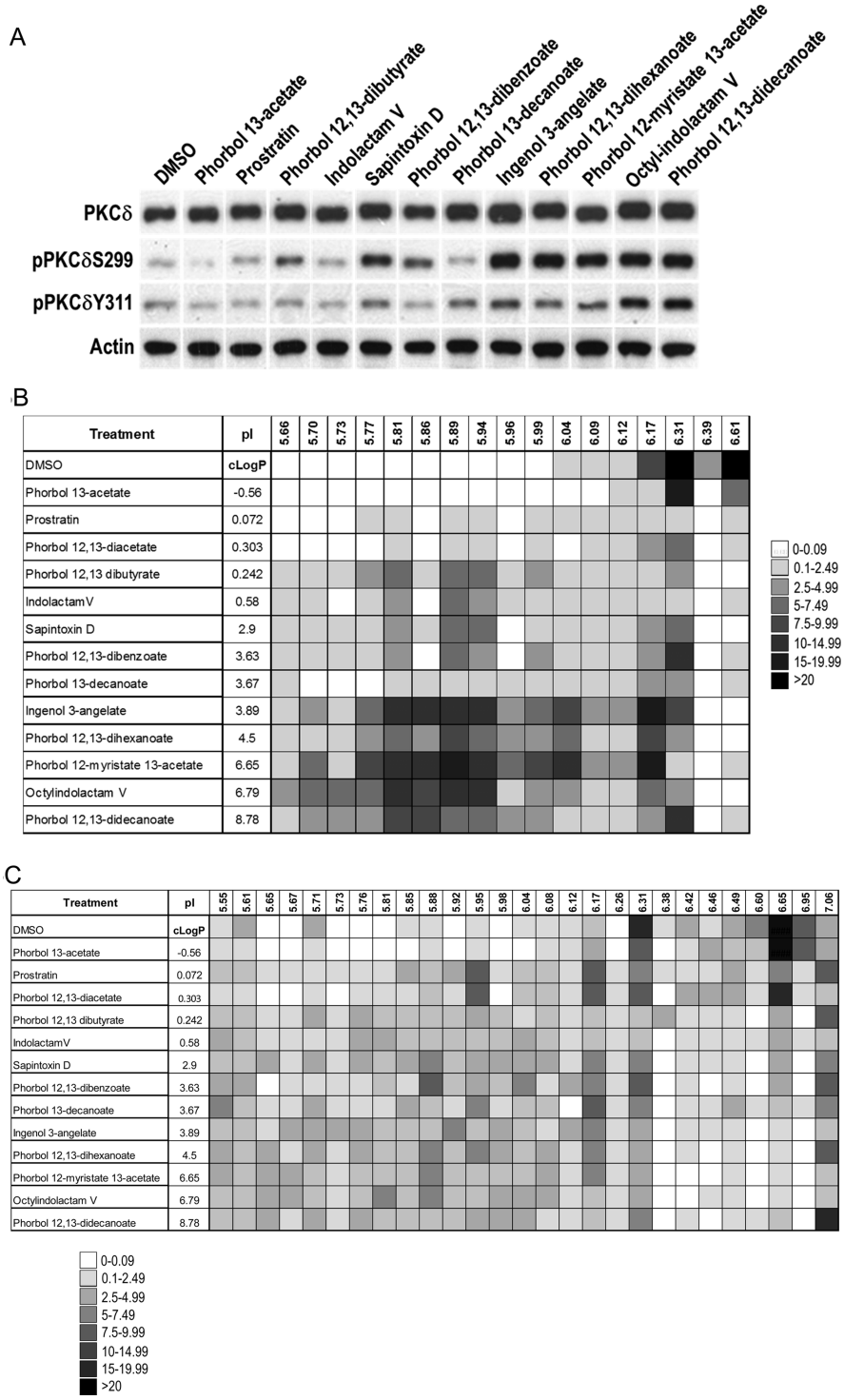

Figure 5. The pattern of PKCδ modification is different for different PKC ligands. LNCaP cells were treated with different PKC activators (10 000 nM for phorbol 13-acetate and prostratin, 1000 nM for others) for 150 min. Total cell lysates were prepared and evaluated by Western blotting (A), by the charge-based Simple Western system using pPKCδS299 antibody (B), or by the charge-based Simple Western system using total PKCδ antibody (C). (A) Immunoblot analysis of total cell lysates using the indicated antibodies. A representative image of three independent experiments is shown. For analysis using the charge-based Simple Western system the areas under peaks were calculated and expressed as % of the total peaks for PMA in the same set of runs (B) or % of total peaks in the sample (C). The heat map represents the average % values for each detected peak (n = 3 except for phorbol 13-acetate, phorbol 12,13-diacetate, phorbol 12,13-dibenzoate, and phorbol 13-decanoate where n = 2). cLogP = calculated log P values using Chemdraw.

specific peaks within the profile were also evident. Thus, peak 6 in the PMA treatment profile was markedly diminished upon bryostatin 1 treatment whereas peak 7 was elevated. Conceptually important, all of these peaks were being detected with the pPKCδS299 antibody, so this single antibody was detecting a multiplicity of different modification states of activated PKCδ, which presumably are not functionally equivalent but which all are combined into a single band on

dx.doi.org/10.1021/jm500417b | J. Med. Chem. 2014, 57, 5356−5369

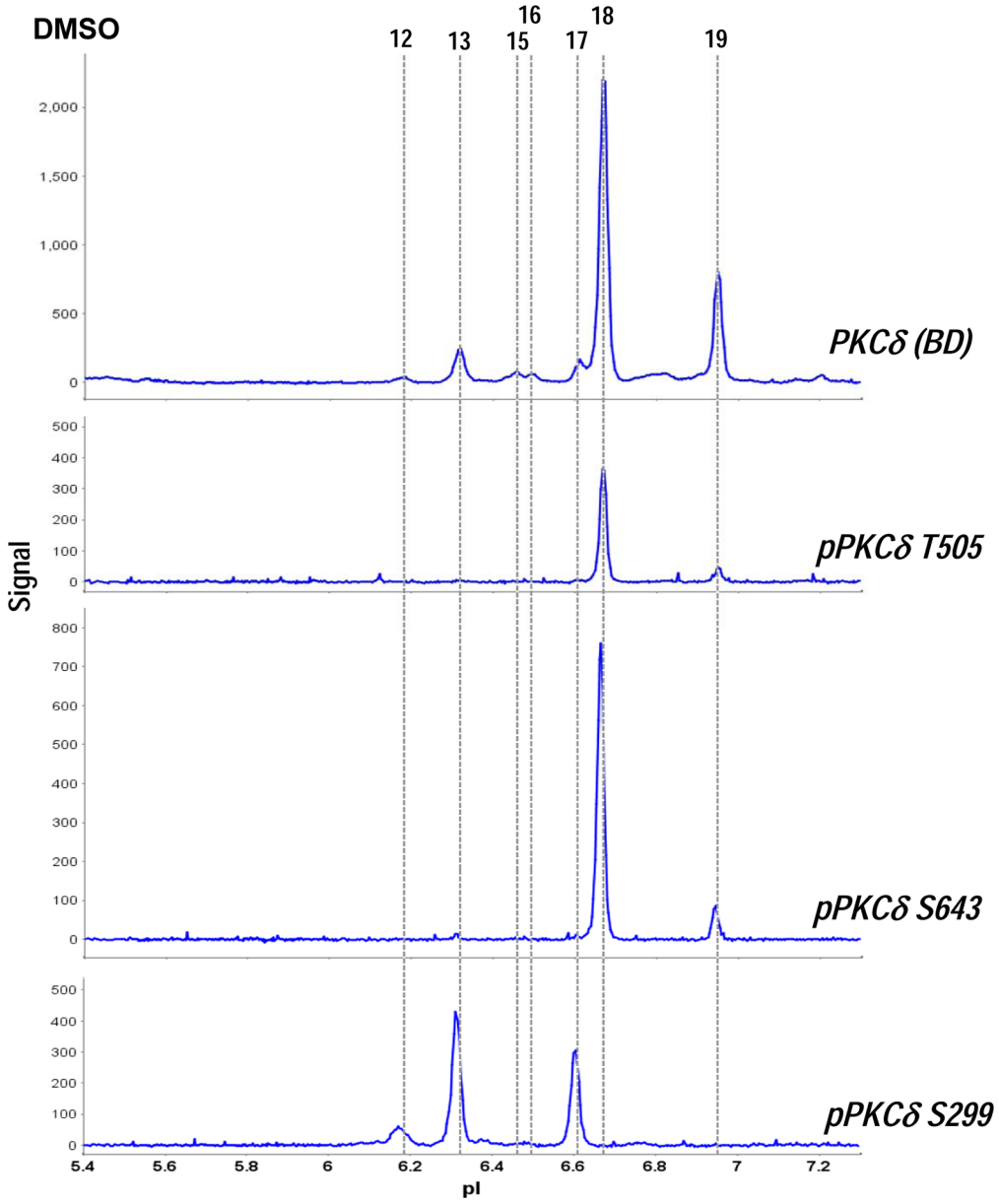

Figure 6. Detection of changes in PKCδ phosphorylation by the charge-based Simple Western system using different PKCδ antibodies. The total cell lysate of DMSO treated LNCaP cells used in Figure 3 was analyzed by the charge-based Simple Western system using the indicated antibodies. The total PKCδ antibody used in this figure was from BD Biosciences. Single experiments were performed with total PKCδ, pPKCδT505, and pPKCδS643.

immunoblotting and interpreted as activated PKCδ. As discussed in more detail later, we do not know the specific modifications accounting for most elements of the isoelectric focusing profiles in the presence of PMA, bryostatin 1, or Merle 23. All the peaks detected with pPKCδS299 would be expected to contain this phosphorylation and most presumably would contain the phosphorylations at the activation loop (T505), the turn motif (S643), and the hydrophobic motif (S662).

Profiles were dependent not only on the ligand but also on the time of treatment. With time, not only is the absolute level of the PKCδ signal diminished but shifts in the pattern are also observed (Figure 4). This was most evident with PMA and least evident with bryostatin 1.

Elsewhere, we have described differences in the extents to which different phorbol esters and related derivatives inhibit proliferation in LNCaP cells or induce tumor necrosis factor α secretion, an important mediator of the inhibitory response.[38] Similarly, tested at concentrations at or above those giving maximal response for these end points, these ligands had different capacities to induce phosphorylation of PKCδ at S299 or Y311 (Figure 5A). We therefore examined this series of compounds for their effects on the PKCδ signature in the LNCaP cells, as detected with the pPKCδS299 antibody (Figure 5B) and total PKCδ antibody (Figure 5C). Levels of individual peaks for the various ligands were expressed as percent of the total PMA signal observed in the case of the pPKCδS299 antibody (to better compare the level of signal activation by different compounds) or as percent of the total signal of that sample in the case of total PKCδ antibody and presented as a heat map (Figure 5B and Figure 5C). The average values $\pm$ SEM of all points on the heat map are presented in Supporting Information (supplementary data 1A

dx.doi.org/10.1021/jm500417b | J. Med. Chem. 2014, 57, 5356−5369

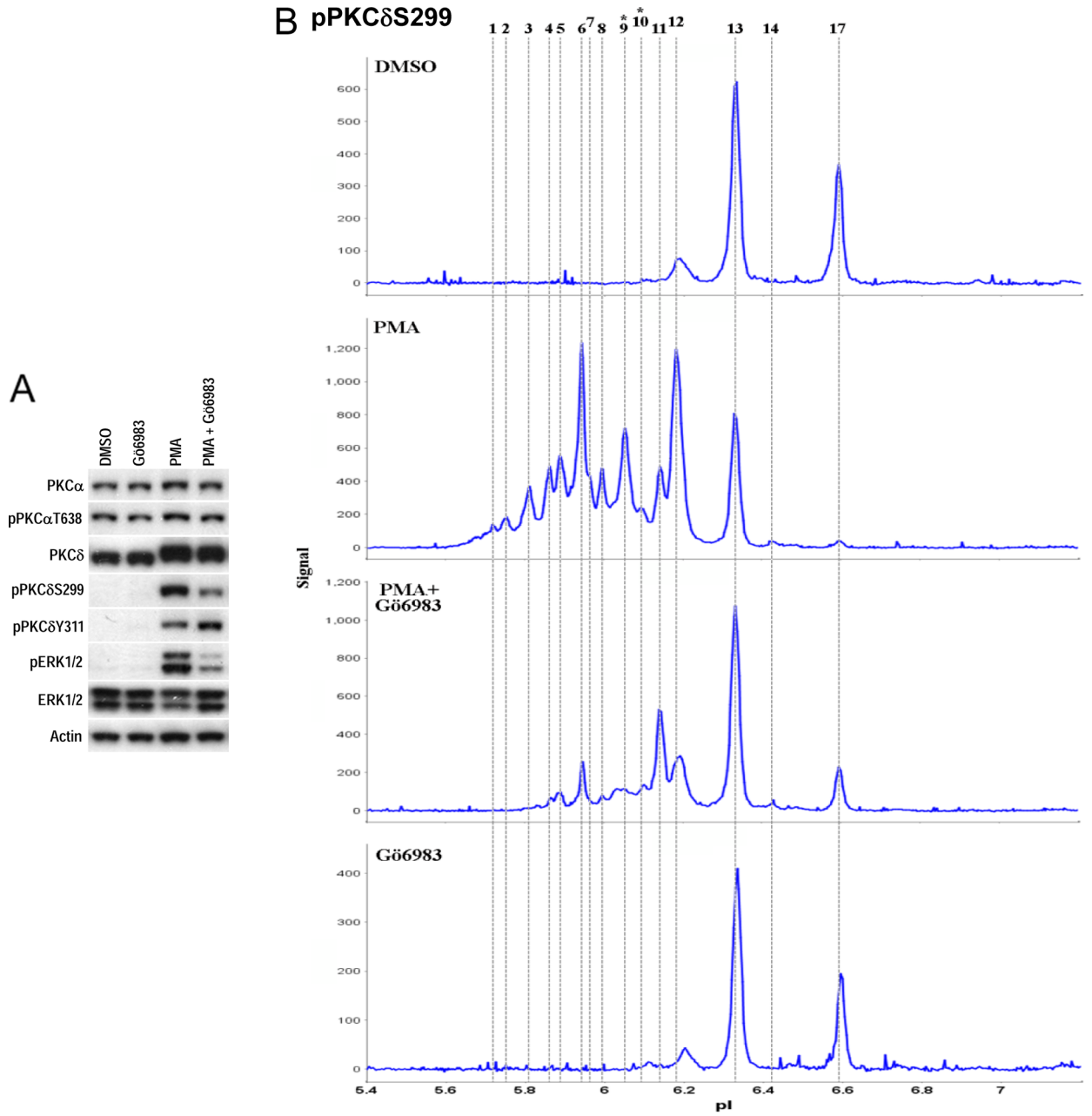

Figure 7. The complex changes in PKCδ phosphorylation are dependent on PKC activity. LNCaP cells were treated with PMA (1000 nM) with or without pretreatment with PKC inhibitor (Gö6983, 3000 nM for 30 min). The total cell lysates were examined by immunoblotting (A) and by the charge-based Simple Western system using pPKCδS299 antibody (B). Data presented are representative of four (A) or two (B) independent experiments. Asterisks in (B) denote that peaks 9 and 10 show variability compared to the peaks labeled 9 and 10 in Figure 3

and 1B). A partial correlation with lipophilicity was observed as well as marked differences among ligands.

Although deconvolution of the various PKCδ modifications responsible for the multiplicity of peaks will be a highly laborious undertaking beyond the scope of the present analysis, it is possible to begin to approach this question using those phospho-specific antibodies that are available (and sensitive enough to detect the responses). This is illustrated for the DMSO control sample, detected with another antibody directed against total PKCδ (antibody from BD Biosciences), as well as those directed against pPKCδT505, pPKCδS643, and pPKCδS299 (Figure 6). The peak profiles detected using the two different total PKCδ antibodies are very similar (Figure 3A, Figure 6, Supporting Information Figure 2). Peaks 18 and 19 detected with the total PKCδ antibody also show phosphorylation on sites T505 and S643 (81.35% of total PKCδ is phosphorylated on T505 and S643), whereas about 12.53% of total PKCδ is phosphorylated at S299 under these basal conditions in this experiment (peaks 12, 13, and 17) (Figure 6). The slide also illustrates that the level of basal PKCδ phosphorylation at S299 showed some variation with different batches of cells (compare Figure 3A and Figure 6). Importantly, the figure illustrates that the relative proportions of the peaks with the antibodies directed against total PKCδ permit an estimate of the relative proportions of the modified peaks, whereas their relative contributions could not be inferred from the absolute signal strengths with the various antibodies. Unfortunately, the sensitivities of the antibodies directed

dx.doi.org/10.1021/jm500417b | J. Med. Chem. 2014, 57, 5356−5369

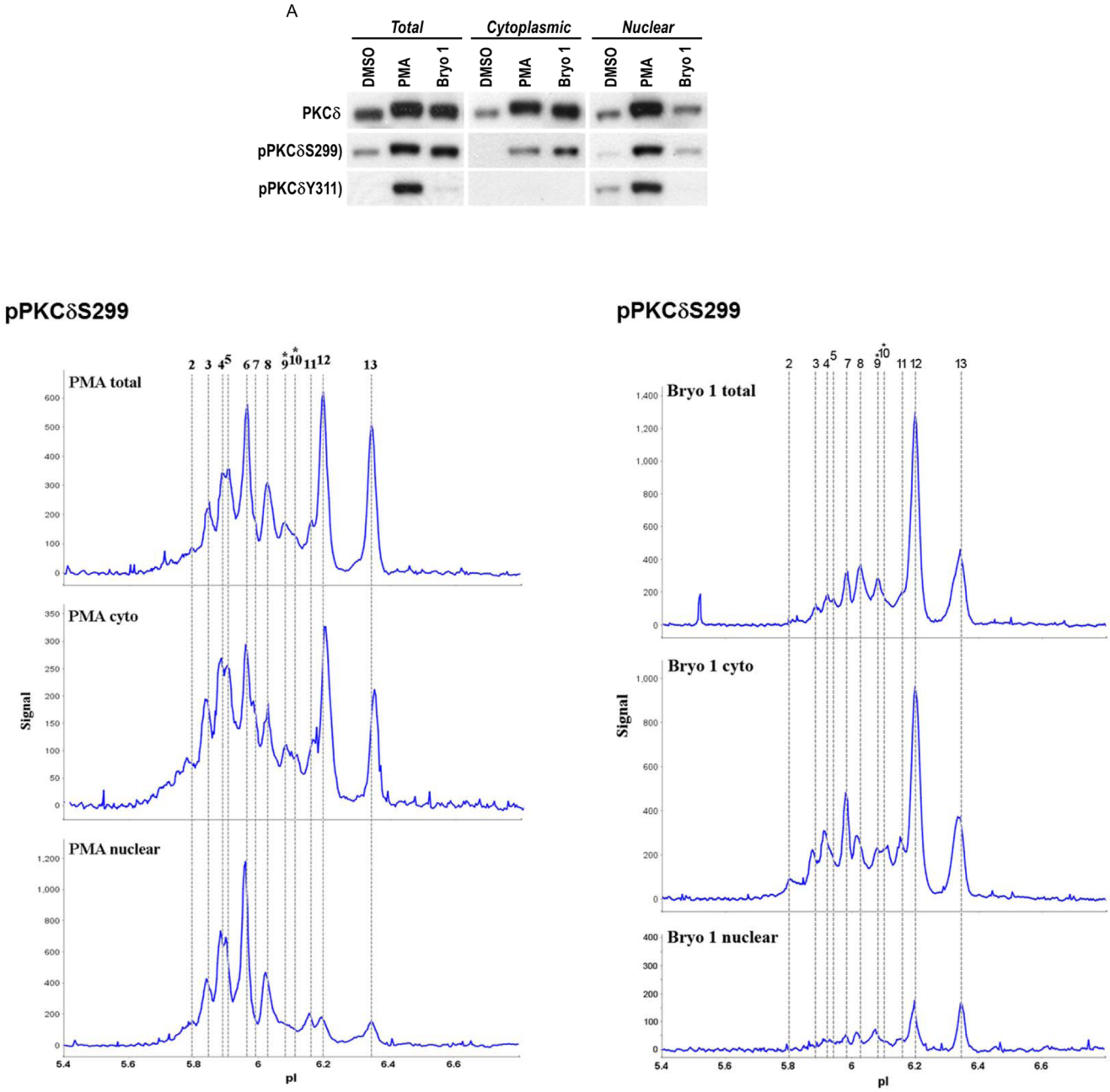

Figure 8. Phosphorylation pattern of PKCδ in different cellular compartments. LNCaP cells were treated for 60 min with PMA, bryostatin 1 (1000 nM), or DMSO as control. Nuclear extracts were prepared. PKCδ phosphorylation in the total cell lysates, the cytoplasmic fraction, and the nuclear fraction was detected by immunoblotting (A) and by the charge-based Simple Western system using the pPKCδS299 antibody (B). Data are representative of three independent experiments. Asterisks in (B) denote that peaks 9 and 10 show variability compared to the peaks labeled 9 and 10 in Figure 3

against T505 and S643 were not adequate for analysis once the PKCδ profile was spread over the multiple bands upon phorbol ester treatment.

To evaluate the role of PKCδ activity in the subsequent phosphorylation changes, we examined the effect of the general PKC inhibitor Gö6983 (3000 nM) on the phosphorylation response. Under these conditions, this concentration of Gö6983 largely but not entirely blocked the PMA stimulated PKC activity, as revealed by immunoblotting (Figure 7A), with a reduction in ERK1/2 phosphorylation and pPKCδS299 staining. By charge-based Simple Western analysis, treatment with Gö6983 alone had no effect on the pattern of peaks (Figure 7B). In contrast, a marked reduction in the overall magnitude of the profile from the PMA stimulated cells was observed upon detection with the pPKCS299 antibody with the residual bands predominantly at higher pI.

We have described earlier that treatment with PMA or bryostatin 1 causes different distribution between a nuclear enriched fraction and the cytoplasm.[33] We confirm here that PMA treatment causes enhanced phosphorylation on Y311 of PKCδ and this species is predominantly found in the nuclear enriched fraction (Figure 8A). Likewise, the pS299 signal upon PMA treatment is predominantly in the nuclear enriched fraction whereas that upon bryostatin 1 treatment is

dx.doi.org/10.1021/jm500417b | J. Med. Chem. 2014, 57, 5356−5369

predominantly in the cytoplasmic fraction (Figure 8A). Analysis by the charge-based Simple Western system emphasizes the difference in the profile of PKCδ between these two fractions, with the nuclear enriched fraction enriched in the lower pI forms upon PMA treatment, which is not observed with Bryo 1 treatment (Figure 8B). This is particularly evident upon detection with the pPKCδS299 antibody. The pPKCδY311 antibody did not yield a sufficiently strong signal for analysis of the multiple bands generated upon phorbol ester treatment. Although we do not know if phosphorylation at S299 and at Y311 are found in some of the same peaks, it seems highly likely that they would be at least partially coincident because Y311 phosphorylation is associated with PKCδ that is active[15,16] and S299 phosphorylation presumably reflects the active conformation of the PKCδ exposing the hinge region, where S299 is located.[23]

Only Minor Differences in Regulation of PKCα by Ligands As Detected by Analysis Using the Charge-Based Simple Western System. In marked contrast to the complex pattern of modification of PKCδ upon ligand addition, analysis of PKCα by the charge-based Simple Western system showed only minor changes. A single prominent band was evident in the DMSO control. Treatment with PMA, bryostatin 1, or Merle 23 caused similar, quantitatively minor changes with the appearance of three bands at lower pI (Figure 9). The same simple pattern was detected with the PKCα antibody from Epitomics (data not shown).

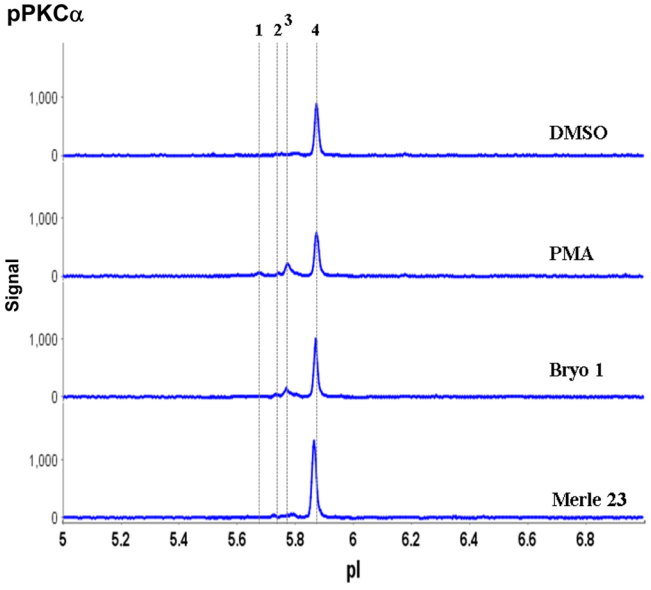

Figure 9. Simple phosphorylation pattern of PKCα measured by the charge-based Simple Western system. The total cell lysates used in Figure 3 were evaluated by the charge-based Simple Western system using PKCα antibody (Santa Cruz). The results are representative of three independent experiments.

DISCUSSION

Our findings have impact at multiple levels. We find that different C1 domain-targeted PKC ligands have qualitatively different effects on PKC phosphorylation (or other modifications affecting the isoelectric point). The isoelectric focusing signature can thus be used as a guide to synthesis, reporting how congeners may retain or diverge in their pattern of action, as reflected through this signature. The charge-based Simple Western resolution of PKCδ isoelectric states revealed both the great complexity and extensiveness of PKCδ modification. Finally, our analysis of PKCδ provided an initial glimpse into the methodological issues and exciting potential of the approach.

It is essential to emphasize that the isoelectric focusing patterns obtained yield a signature for PKCδ modification. Individual peaks within the pattern may represent several combinations of phosphorylation events, provided that each combination results in the same isoelectric point for the protein. Indeed, although the individual peaks are interpreted for convenience as representing different phosphorylation states of PKCδ, the results could also incorporate any changes in isoelectric point arising through other mechanisms. Although degradation cannot be excluded as a contributor to such complexity, we failed to see significant degradation at these early times of treatment upon size fractionation on SDS polyacrylamide gels, either as a decrease in the signal at the size of the intact protein or as the appearance of lower molecular weight bands under our detection conditions. In any case, while we have developed some insights through the use of antibodies of different specificities, full deconvolution of the identities of the combinations of underlying sites and types of modifications constitutes a formidable future challenge. That was not our objective here. Just as patterns of gene expression provide a signature of the systems biology of a cell or tissue, with different signatures being associated with different underlying perturbations of cellular control,[40,41] so the pattern of modification of protein kinase Cδ provides a signature for the integrated consequences of activation, of autophosphorylation, of heterophosphorylation by both serine/threonine specific kinases and tyrosine kinases, and of dephosphorylation by phosphatases. These in turn will have been influenced not only by PKCδ activation but also by changes in its subcellular localization and interaction with anchoring proteins as well as the kinetics of these changes. Speculatively, a further potential element may be intermediate conformational states of PKC. In the case of PKC βII, recent elegant crystallographic studies indicate that one of the twin C1 domains, the C1b domain, is involved in intramolecular contacts with the kinase domain.[42] Abundant evidence suggests different structure−activity relations for the two C1 domains,[43,44] and occupancy of just one C1 domain may yield a different conformation for PKC than does occupancy of both.

The LNCaP cells show very complicated behavior in response to treatment with phorbol esters or related derivatives. In response to the typical phorbol ester phorbol 12-myristate 13-acetate (PMA), the cells show growth inhibition and apoptosis.[45,46] This response reflects both stimulation of secretion of tumor necrosis factor α and modulation of downstream signaling.[47] Like PMA, bryostatin 1 binds to the C1 domains of PKC and leads to PKC activation. Paradoxically, however, bryostatin 1 fails to induce many of the responses typically induced by the phorbol esters, and for those responses that it fails to induce, it inhibits response to the phorbol ester upon cotreatment.[30] Correspondingly, in the LNCaP cells bryostatin 1 fails to inhibit cell growth and induces only minimal tumor necrosis factor α secretion.[33,48] PKCδ appears to be the primary PKC isoform determining the outcome in this system. This is consistent with our finding that the expression level of PKCδ is at least 20 times higher than other PKC isoforms in LNCaP cells.[49]

dx.doi.org/10.1021/jm500417b | J. Med. Chem. 2014, 57, 5356−5369

Bryostatin 1 is of great interest as a therapeutic agent for cancer[50] and dementia,[51] as reflected in multiple clinical trials. Because of the formidable obstacles to supply of this complex natural product,[52] there has been intense interest in the development of synthetic congeners, retaining the same pattern of biological activity as bryostatin 1 while eliminating those structural features that complicate synthesis but are unnecessary for activity.[39] Using the LNCaP cell system as a potential cellular model for evaluating such congeners, we found that the simplified synthetic bryostatin 1 derivative Merle 23[32] appeared to act like bryostatin 1 in this system, failing to inhibit proliferation and stimulating only a low level of tumor necrosis factor α secretion.[33] Further examination of the behavior of Merle 23 in the LNCaP cells, however, revealed appreciable differences between it and bryostatin 1. For example, addition of a proteosome inhibitor shifted the behavior of Merle 23 to that of PMA, whereas the response to bryostatin 1 remained largely the same. In further studies, we showed that a series of other phorbol esters and indolactams likewise did not all behave like PMA but showed variable extents of lesser response, in partial similarity to bryostatin 1.[38] Analysis in the LNCaP cells of compounds drawn from this series thus seemed well suited for detecting potential differences in PKCδ phosphorylation in response to different ligands.

Consistent with the different patterns of biological response, we observed that different ligands indeed caused different signatures of modification of PKCδ (as summarized in Figure 5B). Consistent with the response to Merle 23 not fully resembling that to bryostatin 1, we observed an intermediate pattern of modification. It was also clear that, considering all of the ligands, the patterns could not be simply ordered in parallel with their extents of induction of tumor necrosis factor α or inhibition of proliferation. For example, indolactam V was among the most effective for growth inhibition of the LNCaP cells whereas sapintoxin D was among the least effective.[38] Conversely, phorbol 13-decanoate and phorbol 12-myristate 13-acetate showed similar maximal levels of growth inhibition.[38] We suggest that examination of PKCδ isoelectric focusing signatures for mimicry of the pattern observed for bryostatin 1 may afford a stringent test for synthetic bryostatin derivatives that capture its unique pattern of biological response.

One striking aspect of the difference between the effects of PMA and bryostatin 1 was the presence upon PMA treatment of the more acidic PKCδ bands, as detected with the pPKCδS299 antibody, in the nuclear extract fraction. While this nuclear extract fraction was not characterized in detail and thus could also include some other cellular elements, it showed dramatic contrast between the effects of PMA and bryostatin 1. We have speculated that this difference between PMA and bryostatin 1 may be an important contributor to the differential action of these two agents.[33]

Although our goal was to compare signatures of phosphorylation (plus other modifications of isoelectric point) rather than to identify the particular sets of phosphorylated residues represented by each peak, we were able to develop some insights by comparison of the patterns detected with antibodies directed against total PKCδ and against PKC phosphorylated at S299, T505, and Ser643. pS299 has been described as a marker of PKCδ activation in response to ligand binding.[23] pT505 represents phosphorylation of the activation loop, leading to PKCδ being converted to a more active state, and pS643 represents phosphorylation of the turn motif.[22] We could detect and quantify a basal level of S299 phorphorylation in the absence of external activation. While not characterized in detail, this basal S299 phosphorylated PKCδ displayed a lower pI consistent with additional phosphorylations, presumably those at the activation loop, the turn motif, and the hydrophobic motif. Although Y311 phosphorylation would have been of particular interest to evaluate, the quality of pY311 antibodies was not sufficient for analysis with the charge-based Simple Western system.

Although the focus of our analyses was PKCδ, since this residue has been centrally implicated in the unique patterns of response to bryostatin 1 both in LNCaP cells[48,33] and in other systems,[30] we conducted an initial examination of the response of PKCα, one of the other functionally important PKC isoforms in the LNCaP cells. In comparison with PKCδ, the pattern of ligand induced phosphorylation was markedly less complex. A similar situation was observed for PKD1, a kinase that is positionally regulated through its intrinsic C1 domains as well as activated by phosphorylation by PKC isoforms.[53] The complexity of PKCδ phosphorylation is yet another example of its exceptional behavior among PKC isoforms, along with its differential localization by different ligands[8] and the function of its C2 domain as a novel phosphotyrosine binding motif.[54] One potential basis for its complexity of phosphorylation could be through complex formation of PKCδ with other kinases. Through its C2 domain it can bind to phosphotyrosine residues on other kinases;[54] through its own phosphotyrosine groups it could interact with kinases possessing SH2 domains; through either mechanism it further could interact with adapter proteins bringing it into proximity with other kinases. The particular value of the isoelectric focusing signatures enabled by the charge-based Simple Western system for analysis of contextual structure−activity relationships probably lies in targets such as PKCδ, which reflect such complexity.

The current analysis of PKCδ response to ligands using the charge-based Simple Western system represents an early stage in the evaluation of the utility of this approach. Signatures such as observed in the treated cellular systems could be extended to define signatures in dissected tumor samples, reporting on signaling pathway regulation in the tissue sample. Modifications, such as the use of a validated detection tag, which could be coupled to any target of interest, would facilitate its generalized application to a wide range of targets, without needing to identify and validate specific antibodies for each target. Use of a fluorescent tag might simplify detection. An efficient system for subsequent identification of the specific sites of phosphorylation represented would move the analysis to the next step from response signature toward dissected phosphorylation pathway. Nonetheless, the methodology has already proven to be highly informative for our understanding of PKCδ pharmacology and regulation.

EXPERIMENTAL SECTION

Materials. All phorbol esters were purchased from LC Laboratories (Woburn, MA) unless otherwise specified (purity for all >99%). Sapintoxin D (purity >98% by HPLC) was from Enzo Life Sciences International Inc. (Plymouth Meeting, PA). Bryostatin 1 was provided by the Developmental Therapeutics Program, NCI (Frederick, MD). Bryostatin 1 was judged to be greater than or equal to 95% purity, as determined by ^{1}H and ^{13}C NMR, as well as HPLC analysis. The synthesis of Merle 23 was described earlier.[32] Merle 23 was isolated as single observable TLC spot in 40% EtOAc/hexanes, appeared as a single peak by reverse phase HPLC using a Waters 4.5 μm × 150 μm

dx.doi.org/10.1021/jm500417b | J. Med. Chem. 2014, 57, 5356−5369

C18 column and was judged to be >95% pure by 500 MHz ^{1}H NMR and 125 MHz ^{13}C NMR.

The LNCaP human prostate cancer cell line, fetal bovine serum (FBS), and RPM1-1640 medium were obtained from ATCC (Manassas, VA). Precast 10% SDS gels and PBS were from Invitrogen (Carlsbad, CA). The primary antibody against PKCα (sc-208) was from Santa Cruz Biotechnology (Santa Cruz, CA) and that against PKCδ was from Santa Cruz Biotechnology (sc-937) or BD Biosciences (San Jose, CA). The primary antibodies against phosphorylated PKCδ (pPKCδY311, pPKCδT505, pPKCδS643) and phosphorylated PKCα (pPKCαT638), pERK1/2 (no. 9101), and ERK1/2 (no. 9102) were from Cell Signaling (Danvers, MA). Those against PKCα (no. 1510-1), PKCδ (no. 2222-1), and phosphorylated PKCδ (pPKCδS299 and another antibody against pPKCδY311) were from Epitomics (Burlingame, CA). The mouse monoclonal antibody against β-actin was from Sigma (St. Louis, MO). The horseradish peroxidase conjugated secondary anti-rabbit antibodies, the nonfat dry milk, Tween-20, and the Triton X-100 solution were from Bio-Rad (Hercules, CA). The ECL (electrochemiluminescence) reagent and the films were from GE Healthcare (Piscataway, NJ). The following reagents were from ProteinSimple (Santa Clara, CA): 1× fluorescent pI standard 6.4, 7.0 and ladder 4 (no. 040-030, no. 040-031, and no. 040-647, respectively), 1× G2 premix 5-8 ampholyte (no. 040-973), Luminol (no. 040-652), and peroxide (no. 041-084). The secondary goat anti-rabbit antibody (no. 111-035-144) and donkey anti-mouse antibody (no. 715-035-150) used for charge-based Simple Western analysis were from Jackson ImmunoResearch (West Grove, PA).

Methods. Cell culture, treatment of cells, preparation of total cells lysates and nuclear extracts, and the Western blotting were performed as described earlier.[33]

Analysis by Charge Based Simple Western. Except for cell fractionation samples, cells were lysed with RIPA buffer (20 mM HEPES, pH 7.5, 150 mM NaCl, 1% NP 40 alternative, 0.25% sodium deoxycholate) containing phosphatase and protease inhibitors (EMD Millipore catalog no. 524624 and no. 539134, respectively). Cell lysates (approximately 20 ng of protein) were mixed with 1× G2 premix 5-8 ampholyte, and 1× fluorescent pI standard 6.4, 7.0, and ladder 4 before being loaded into the NanoPro1000 system (ProteinSimple, Santa Clara, CA) for analysis. During isoelectric focusing electrophoresis, proteins were separated by charge and concentrated at their respective isoelectric focusing points in the capillaries. Separated proteins were immobilized on the capillary wall using UV light, followed by immunoprobing with the indicated primary antibodies and HRP-conjugated goat anti-rabbit (1:100 diluted) or donkey anti-mouse (1:100 diluted) secondary antibody. The primary antibodies used in the study were the following: pPKCδS299 (1:50 diluted), PKCδ (1:100 diluted, Santa-Cruz sc-937), PKCα (1:50 diluted, Santa-Cruz sc-208), PKCδ (1:100 diluted, BD Biosciences no. 610397), pPKCδT505 (1:50 diluted, Cell Signaling no. 9374), and pPKCδS643 (1:50 diluted, Cell Signaling no. 9376). Luminol and peroxide were added to generate chemiluminescence, which was captured by a CCD camera. The digital image was analyzed by Compass software (ProteinSimple, Santa Clara, CA). Signal strength is presented as peak area and quantitated. The software calculates the height and area under the curve (AUC) of the separated/individual peaks. For quantitative analysis of PKCδ signals the AUC value of peaks was expressed as % of total AUC (sum of AUC of all peaks for that sample). For pPKCδS299 signals the AUC of individual peaks was expressed as % of total AUC of the PMA treated sample from the same set of runs to reflect the differences in PKCδ activation induced by the different treatments.

■ ASSOCIATED CONTENT

Ⓢ Supporting Information

PKCδ profile in control LNCaP cells detected by two different antibodies by charge-based Simple Western system and the quantitation of the charge-based Simple Western data after treatment of LNCaP cells with different ligands. This material is available free of charge via the Internet at http://pubs.acs.org.

■ AUTHOR INFORMATION

Corresponding Author

*Phone: 301-496-3189. Fax: 301-496-8709. E-mail: blumberp@dc37a.nci.nih.gov.

Author Contributions

$^{\perp}$N.K. and J.-Q.C. contributed equally.

The manuscript was written through contributions of all authors. All authors have given approval to the final version of the manuscript.

Notes

The authors declare no competing financial interest.

■ ACKNOWLEDGMENTS

This research was supported in part by the Intramural Research Program, National Institutes of Health, Center for Cancer Research, National Cancer Institute (Grant Z1A BC 005270) and in part by Grant GM28961 to G.E.K.

■ ABBREVIATIONS USED

CSAR, contextual structure−activity relationship; DAG, *sn*-1,2-diacylglycerol; FBS, fetal bovine serum; FRET, fluorescence resonance energy transfer; GFP, green fluorescent protein; IEF, isoelectric focusing; PKC, protein kinase C; PMA, phorbol 12-myristate 13-acetate

■ REFERENCES

(1) Kazanietz, M. G. *Protein Kinase C in Cancer Signaling and Therapy*; Humana Press: New York, 2010.

(2) Newton, A. C. Protein kinase C: poised to signal. *Am. J. Physiol.: Endocrinol. Metab.* **2010**, *298*, E395−402.

(3) Griner, E. M.; Kazanietz, M. G. Protein kinase C and other diacylglycerol effectors in cancer. *Nat. Rev. Cancer* **2007**, *7*, 281−294.

(4) Zhang, G.; Kazanietz, M. G.; Blumberg, P. M.; Hurley, J. H. Crystal structure of the cys2 activator-binding domain of protein kinase C delta in complex with phorbol ester. *Cell* **1995**, *81*, 917−924.

(5) Hurley, J. H.; Newton, A. C.; Parker, P. J.; Blumberg, P. M.; Nishizuka, Y. Taxonomy and function of C1 protein kinase C homology domains. *Protein Sci.* **1997**, *6*, 477−480.

(6) Marquez, V. E.; Blumberg, P. M. Synthetic diacylglycerols (DAG) and DAG-lactones as activators of protein kinase C (PK-C). *Acc. Chem. Res.* **2003**, *36*, 434−443.

(7) Ma, D.; Tang, G.; Kozikowski, A. P. Synthesis of 7-substituted benzolactam-V8s and their selectivity for protein kinase C isozymes. *Org. Lett.* **2002**, *4*, 2377−2380.

(8) Wang, Q. J.; Bhattacharyya, D.; Garfield, S. H.; Nacro, K.; Marquez, V. E.; Blumberg, P. M. Differential localization of protein kinase C delta by phorbol esters and related compounds using a fusion protein with green fluorescent protein. *J. Biol. Chem.* **1999**, *274*, 37233−37239.

(9) Wang, Q. J.; Fang, T. W.; Fenick, D.; Garfield, S. H.; Bienfait, B.; Marquez, V. E.; Blumberg, P. M. The lipophilicity of phorbol esters as a critical factor in determining the pattern of translocation of protein kinase C delta fused to green fluorescent protein. *J. Biol. Chem.* **2000**, *275*, 12136−12146.

(10) Duan, D.; Sigano, D. M.; Kelley, J. A.; Lai, C. C.; Lewin, N. E.; Kedei, N.; Peach, M. L.; Lee, J.; Abeyweera, T. P.; Rotenberg, S. A.; Kim, H.; Kim, Y. H.; El Kazzouli, S.; Chung, J. U.; Young, H. A.; Young, M. R.; Baker, A.; Colburn, N. H.; Haimovitz-Friedman, A.; Truman, J. P.; Parrish, D. A.; Deschamps, J. R.; Perry, N. A.; Surawski, R. J.; Blumberg, P. M.; Marquez, V. E. Conformationally constrained analogues of diacylglycerol. 29. Cells sort diacylglycerol-lactone chemical zip codes to produce diverse and selective biological activities. *J. Med. Chem.* **2008**, *51*, 5198−5220.

(11) Freeley, M.; Kelleher, D.; Long, A. Regulation of protein kinase C function by phosphorylation on conserved and non-conserved sites. *Cell. Signalling* **2011**, *23*, 753−762.
(12) Newton, A. C. Regulation of the ABC kinases by phosphorylation: protein kinase C as a paradigm. *Biochem. J.* **2003**, *370*, 3261−3271.
(13) Rosse, C.; Linch, M.; Kermorgant, S.; Cameron, A. J. M.; Boeckeler, K.; Parker, P. J. PKC and the control of localized signal dynamics. *Nat. Rev. Mol. Cell Biol.* **2010**, *11*, 103−112.
(14) Gould, C. M.; Newton, A. C. The life and death of protein kinase C. *Curr. Drug Targets* **2008**, *9*, 614−625.
(15) Steinberg, S. F. Structural basis of protein kinase C isoform function. *Physiol. Rev.* **2008**, *88*, 1341−1378.
(16) Steinberg, S. F. Distinctive activation mechanisms and functions for protein kinase C delta. *Biochem. J.* **2004**, *384*, 449−459.
(17) Brodie, C.; Blumberg, P. M. Regulation of cell apoptosis by protein kinase C delta. *Apoptosis* **2003**, *8*, 19−27.
(18) Reyland, M. E. Protein kinase C delta and apoptosis. *Biochem. Soc. Trans.* **2007**, *35*, 1001−1004.
(19) Blass, M.; Kronfeld, I.; Kazimirsky, G.; Blumberg, P. M.; Brodie, C. Tyrosine phosphorylation of protein kinase C delta is essential for its apoptotic effect in response to etoposide. *Mol. Cell. Biol.* **2002**, *22*, 182−195.
(20) Zrachia, A.; Dobroslav, M.; Blass, M.; Kazimirsky, G.; Kronfeld, I.; Blumberg, P. M.; Kobiler, D.; Lustig, S.; Brodie, C. Infection of glioma cells with Sindbis virus induces selective activation and tyrosine phosphorylation of protein kinase C delta. Implications for Sindbis virus-induced apoptosis. *J. Biol. Chem.* **2002**, *277*, 23693−23701.
(21) Rybin, V. O.; Guo, J.; Sabri, A.; Elouardighi, H.; Schaefer, E.; Steinberg, S. F. Stimulus-specific differences in protein kinase C delta localization and activation mechanisms in cardiomyocytes. *J. Biol. Chem.* **2004**, *279*, 19350−19361.
(22) Sumandea, M. P.; Rybin, V. O.; Hinken, A. C.; Wang, C.; Kobayashi, T.; Harleton, E.; Sievert, G.; Balke, C. W.; Feinmark, S. J.; Solaro, R. J.; Steinberg, S. F. Tyrosine phosphorylation modifies PKCδ-dependent phosphorylation of cardiac troponin I. *J. Biol. Chem.* **2008**, *283*, 22680−22689.
(23) Durgan, J.; Michael, N.; Totty, N.; Parker, P. J. Novel phosphorylation site markers of protein kinase C delta activation. *FEBS Lett.* **2007**, *581*, 3377−3381.
(24) Welman, A.; Griffiths, J. R.; Whetton, A. D.; Dive, C. Protein kinase C-δ is phosphorylated on five novel Ser/Thr sites following inducible overexpression in human colorectal cancer cells. *Protein Sci.* **2007**, *16*, 2711−2715.
(25) Rybin, V. O.; Guo, J.; Harleton, E.; Feinmark, S. J.; Steinberg, S. F. Regulatory autophosphorylation sites on protein kinase C-delta at threonine-141 and threonine-295. *Biochemistry* **2009**, *48*, 4642−4651.
(26) Brognard, J.; Newton, A. C. PHLiPPing the switch on Akt and protein kinase C signaling. *Trends Endocrinol. Metab.* **2008**, *19*, 223−230.
(27) Kajimoto, T.; Sawamura, S.; Tohyama, Y.; Mori, Y.; Newton, A. C. Protein kinase C{delta}-specific activity reporter reveals agonist-evoked nuclear activity controlled by Src family of kinases. *J. Biol. Chem.* **2010**, *285*, 41896−41910.
(28) Humphries, M. J.; Ohm, A. M.; Schaack, J.; Adwan, T. S.; Reyland, M. E. Tyrosine phosphorylation regulates nuclear translocation of PKC delta. *Oncogene* **2008**, *27*, 3045−3053.
(29) Pettit, G. R. The bryostatins. *Fortschr. Chem. Org. Naturst.* **1991**, *57*, 153−195.
(30) Blumberg, P. M.; Kedei, N.; Lewin, N. E.; Yang, D.; Czifra, G.; Pu, Y.; Peach, M. L.; Marquez, V. E. Wealth of opportunity—the C1 domain as a target for drug development. *Curr. Drug Targets* **2008**, *9*, 641−652.
(31) Hennings, H.; Blumberg, P. M.; Pettit, G. R.; Herald, C. L.; Shores, R.; Yuspa, S. H. Bryostatin 1, an activator of protein kinase C, inhibits tumor promotion by phorbol esters in SENCAR mouse skin. *Carcinogenesis* **1987**, *8*, 1343−1346.
(32) Keck, G. E.; Kraft, M. B.; Truong, A. P.; Li, W.; Sanchez, C. C.; Kedei, N.; Lewin, N. E.; Blumberg, P. M. Convergent assembly of highly potent analogues of bryostatin 1 via pyran annulation: bryostatin look-alikes that mimic phorbol ester function. *J. Am. Chem. Soc.* **2008**, *130*, 6660−6661.
(33) Kedei, N.; Telek, A.; Czap, A.; Lubart, E. S.; Czifra, G.; Yang, D.; Chen, J.; Morrison, T.; Goldsmith, P. K.; Lim, L.; Mannan, P.; Garfield, S. H.; Kraft, M. B.; Li, W.; Keck, G. E.; Blumberg, P. M. The synthetic bryostatin analog Merle 23 dissects distinct mechansims of bryostatin activity in the LNCaP human prostate cancer cell line. *Biochem. Pharmacol.* **2011**, *81*, 1296−1308.
(34) Markou, T.; Yong, C. S.; Sugden, P. H.; Clerk, A. Regulation of protein kinase C δ by phorbol ester, endothelin-1, and platelet-derived growth factor in cardiac myocytes. *J. Biol. Chem.* **2006**, *281*, 8321−8331.
(35) O'Neill, R. A.; Bhamidipati, A.; Bi, X.; Deb-Basu, D.; Cahill, L.; Ferrante, J.; Gentalen, E.; Glazer, M.; Gossett, J.; Hacker, K.; Kirby, C.; Knittle, J.; Loder, R.; Mastroieni, C.; Maclaren, M.; Mills, T.; Nguyen, U.; Parker, N.; Rice, A.; Roach, D.; Suich, D.; Voehringer, D.; Voss, K.; Yang, J.; Yang, T.; Vander Horn, P. B. Isoelectric focusing technology quantifies protein signaling in 25 cells. *Proc. Natl. Acad. Sci. U.S.A.* **2006**, *103*, 16153−16158.
(36) Fan, A. C.; Deb-Basu, D.; Orban, M. W.; Gotlib, J. R.; Natkunam, Y.; O'Neill, R.; Padua, R. A.; Xu, L.; Taketa, D.; Shirer, A. E.; Beer, S.; Yee, A. X.; Voehringer, D. W.; Felsher, D. W. Nanofluidic proteomic assay for serial analysis of oncoprotein activation in clinical specimens. *Nat. Med.* **2009**, *15*, 566−571.
(37) Chen, J. Q.; Lee, J. H.; Herrmann, M. A.; Park, K. S.; Heldman, M. R.; Goldsmith, P. K.; Wang, Y.; Giaccone, G. *Mol. Cancer Ther.* **2013**, *12*, 2601−2613.
(38) Kedei, N.; Lubart, E. S.; Lewin, N. E.; Telek, A.; Lim, L.; Mannan, P.; Garfield, S. H.; Kraft, M. B.; Keck, G. E.; Kolusheva, S.; Jelinek, R.; Blumberg, P. M. Some phorbol esters may partially resemble bryostatin 1 in their actions on LNCaP prostate cancer cells and U937 leukemia cells. *ChemBioChem* **2011**, *12*, 1242−1251.
(39) Wender, P. A.; Miller, B. L. Synthesis at the molecular frontier. *Nature* **2009**, *460*, 197−201.
(40) Deeb, K. K.; Michalowska, A. M.; Yoon, C.; Krummey, S. M.; Hoenerhoff, M. J.; Kavanaugh, C.; Li, M. C.; Demayo, F. J.; Linnoila, I.; Deng, C. X.; Lee, E. Y.; Medina, D.; Shih, J. H.; Green, J. E. Identification of an integrated SV40 T/t-antigen cancer signature in aggressive human carcinomas with poor prognosis. *Cancer Res.* **2007**, *67*, 8065−8080.
(41) Watters, J. W.; Roberts, C. J. Developing gene expression signatures of pathway deregulation in tumors. *Mol. Cancer Ther.* **2006**, *5*, 2444−2449.
(42) Leonard, T. A.; Rozycki, B.; Saidi, L. F.; Hummer, G.; Hurley, J. H. Crystal structure and allosteric activation of protein kinase C βII. *Cell* **2011**, *144*, 55−66.
(43) Irie, K.; Nakagawa, Y.; Ohigashi, H. Indolactam and benzolactams compounds as new medicinal leads with binding selectivity for C1 domains of protein kinase C isozymes. *Curr. Pharm. Des.* **2004**, *10*, 1371−1385.
(44) Bogi, K.; Lorenzo, P. S.; Szállási, Z.; Acs, P.; Wagner, G. S.; Blumberg, P. M. Differential selectivity of ligands for the C1a and C1b phorbol ester binding domains of protein kinase C delta: possible correlation with tumor-promoting activity. *Cancer Res.* **1998**, *58*, 1423−1428.
(45) Young, C. Y.; Murtha, P. E.; Zhang, J. Tumor-promoting phorbol ester-induced cell death and gene expression in a human prostate adenocarcinoma cell line. *Oncol. Res.* **1994**, *6*, 203−210.
(46) Powell, C. T.; Brittis, N. J.; Stec, D.; Hug, H.; Heston, W. D.; Fair, W. R. Persistent membrane translocation of protein kinase C alpha during 12-0-tetradecanoylphorbol-13-acetate-induced apoptosis of LNCaP human prostate cancer cells. *Cell Growth Differ.* **1996**, *7*, 419−428.
(47) Gonzalez-Guerrico, A. M.; Kazanietz, M. G. Phorbol ester-induced apoptosis in prostate cancer cells via autocrine activation of the extrinsic apoptotic cascade: a key role for protein kinase C delta. *J. Biol. Chem.* **2005**, *280*, 38982−38991.

(48) Von Burstin, V. A.; Xiao, L.; Kazanietz, M. G. Bryostatin inhibits phorbol ester-induced apoptosis in prostate cancer cells by differentially modulating protein kinase C (PKC) delta translocation and preventing PKC delta-mediated release of tumor necrosis factor-alpha. *Mol. Pharmacol.* **2010**, *78*, 325−332.
(49) Chen, J. Q.; Heldman, M. R.; Herrmann, M. A.; Kedei, N.; Woo, W.; Blumberg, P. M.; Goldsmith, P. K. Absolute quantitation of endogenous proteins with precision and accuracy using a capillary Western system. *Anal. Biochem.* **2013**, *442*, 97−103.
(50) Kortmansky, J.; Schwartz, G. K. Bryostatin-1: a novel PKC inhibitor in clinical development. *Cancer Invest.* **2003**, *21*, 924−936.
(51) Sun, M. K.; Alkon, D. L. Bryostatin-1: pharmacology and therapeutic potential as a CNS drug. *CNS Drug Rev.* **2006**, *12*, 1−8.
(52) Hale, K. J.; Manaviazar, S. New approaches to the total synthesis of the bryostatin antitumor macrolides. *Chem.—Asian J.* **2010**, *5*, 704−754.
(53) Wang, Q. J. PKD at the crossroads of DAG and PKC signaling. *Trends Pharmacol. Sci.* **2006**, *27*, 317−323.
(54) Benes, C. H.; Wu, N.; Elia, A. E.; Dharia, T.; Cantley, L. C.; Soltoff, S. P. The C2 domain of PKC delta is a phosphotyrosine binding domain. *Cell* **2005**, *121*, 158−160.
(55) Konishi, H.; Tanaka, M.; Takemura, Y.; Matsuzaki, H.; Ono, Y.; Kikkawa, U.; Nishizuka, Y. Activation of protein kinase C by tyrosine phosphorylation in response to H_2O_2. *Proc. Natl. Acad. Sci. U.S.A.* **1997**, *94*, 11233−11237.